Water Practice & Technology

IWA PUBLISHING

Water Practice & Technology Vol 18 No 8, 1880 doi: 10.2166/wpt.2023.106

Studying the effect of boiler water releasing in rivers on some water properties (Al-Euphrates River at Al-Mussaib thermal power station as case study)'

Mohsin J. Nasir [a,*], Ahmed Sami Naser[b], Wisam Abdulabbas Abidalla[a] and Ghosoon Natiq Ismael[a]

[a] Al-Mussaib Technical Institute, Al-Furat Al-Awsat Technical University, Babylon 51009, Iraq
[b] Ammara Technical Institute, Southern Technical University, Ammara, Iraq
*Corresponding author. E-mail: inm.mohs@atu.edu.iq

MJN, 0000-0002-9714-3037

ABSTRACT

Studying the effect of boiler water released in rivers on some water properties such as density, viscosity was done in this research. Equations of momentum, conversation, turbulence and energy were used with the relation between the temperature and water properties to describe those properties along the study reach. Simplifying of partial equation was done to obtain system of linear equation. Verification of numerical model by conducting comparison of observed data from Euphrates River at Mussaib Thermal Power Station with those computed by the model. The comparison results of density and viscosity show an agreement with using statistical tests such as Chi square and RMSE. The results of the study showed that increasing the bed roughness from 0.04 m to 0.12 m causes a longitudinal retardation of the values of density and viscosity values about (26 and 22%) respectively and vertical advance of these values about (14 and 12%) respectively. Increasing the water surface slope from (6 cm/km to 12 cm/km) causes a longitudinal advance of density and viscosity values about (19 and 12%) respectively and vertical retardation of these values about (16 and 13%) respectively.

Key words: boiler water, linear equation, numerical model, water properties, water surface slope

HIGHLIGHTS

- Effects of boiler water on water river properties such as water density and water viscosity were studied.
- Significance and degree of freedom between observed data from the river and predicted data from the model were studied.
- The effects of hydraulic river properties such as bed height and water surface slope on distribution of the values of these water river properties were explored.

LIST OF SYMBOLS

X, Z	Horizontal and vertical coordinates respectively (m)
P	Pressure (N/m^2)
g	Acceleration due to gravity (m/s^2)
H	Heat exchange across the water surface kg. °K/(m^2.s)
C_p	Specific heat w.s/(kg. °K)
T	Heated water temperature (°C)
T_r	River water temperature (°C)
K	Turbulent kinetic energy (kg/s)
G	Rate of production of turbulence kinetic energy
$C1$, $C2$	Constants in kinetic energy turbulence model
C_p	Heating capacity (j/kg.K)
V	Velocity (m/s)
h	Water depth measured at Z-axis (m)
S	Slope of the water surface (cm/km)
n	Roughness height (m)
U	Longitudinal velocity components (m/s)
R	Hydraulic radius (m)
G	Acceleration due to gravity (m/s^2)

U_f Friction velocity (m/s)

Greek symbols

ρ Density (kg/m^3)
μ Viscosity (N.s/m^2)
α Heat transfer coefficient (W/(m^2.K)
σ Prandtle number
γ Surface tension (N/m)
ε Dissipation rate (m^2/s^3)
ϕ Thermal flow (W/m^2)
RMSE Root mean square error

1. INTRODUCTION

Discharging boiler water into rivers or any bodies of water causes thermal pollution, which leads to several important effects. River water temperature increases more than normal levels when hydropower discharges boiler water, causing harms to animals and plants living in the water. Physical water properties such as density, viscosity, etc., are affected by temperature change (Babartutsi & Chu 1998). The abnormal process causes thermal pollution and changes the temperature of the surrounding water. Hydropower plants use water for cooling factory elements and the resulting hot water to streams. High water temperatures may be disastrous to the environment by affecting aquatic life such as fish (APHA 2011; Kalinowska & Rowinski 2012). An Environmental Impact Assessment (EIA) is crucially required for establishing such facilities. Among many EIA aspects, the prediction of a potential water temperature rise with the source of artificial heat is of great importance. Using numerical models, the predictions are usually made. Choosing an appropriate model, as well as collecting data to be used as model inputs, are often challenging tasks (APHA 2011). In principle, the predictive calculations should be carried out in dangerous situations from an environmental point of view (Kalinowska & Rowinski 2015; Abidalla *et al.* 2022). The rising river temperatures are an environmental concern so heat pollution is regulated by the Clean Water Act (CWA), which prohibits industrial facilities without permits from raising river temperatures above permissible limits. While previous studies of electricity generation focused on impacts on water resources and climate changes, assessments of thermal pollution had a unifying effect in focusing on the determining of temperature rise in the receiving water (EPA 2001; Macknick *et al.* 2016). The importance of incorporating a higher resolution for an accurate assessment of thermal pollution has also not yet been addressed. Assessments of susceptibility to thermal pollution and electricity generation are typically performed across large fields. Studies using coarse spatial resolution may miscalculate the extent of thermal pollution because they force the placement of multiple plants within a single grid cell and fail to capture subtle differences in the river discharge, temperature and the rates of thermal equilibrium. The rate of thermal equilibrium plays a main role in the river temperature modeling because they determine the natural warming cooling of the river and the longevity of thermal pollution as it moves downstream (Behrens *et al.* 2017; Nasir *et al.* 2022).

Nasir *et al.* (2013) applied a numerical model for studying the distribution of some other water properties caused by discharging of boiler water in rivers. The results showed an increase in the bed roughness and the slope of the water surface, which causes changes in the dissolved oxygen distribution. Miaral *et al.* (2018) evaluated the impact of warming in the Mississippi River as a result of power plant waste. The results showed that the use of coarse river network decisions may lead to a significant exaggeration in estimating the size and length of the weak river tributaries, and therefore necessitates the use of recycled cooling techniques that can reduce thermal pollution, but at the expense of the electric power generation capacity. This study aims to use two-dimensional numerical models to simulate the behavior of water properties, such as density and viscosity, due to released boiler water in the Euphrates River and the effects of the hydraulic conditions in river, such as the bed roughness and slope of watersurface, on the behavior of these properties.

2. MATERIAL AND METHODS

2.1. The study area

The data was collected from the area located at Mussaib city near Al-Mussaib Thermal Power Station on the banks of the Euphrates River in Babylon Governorate, Iraq, as shown in Figure 1.

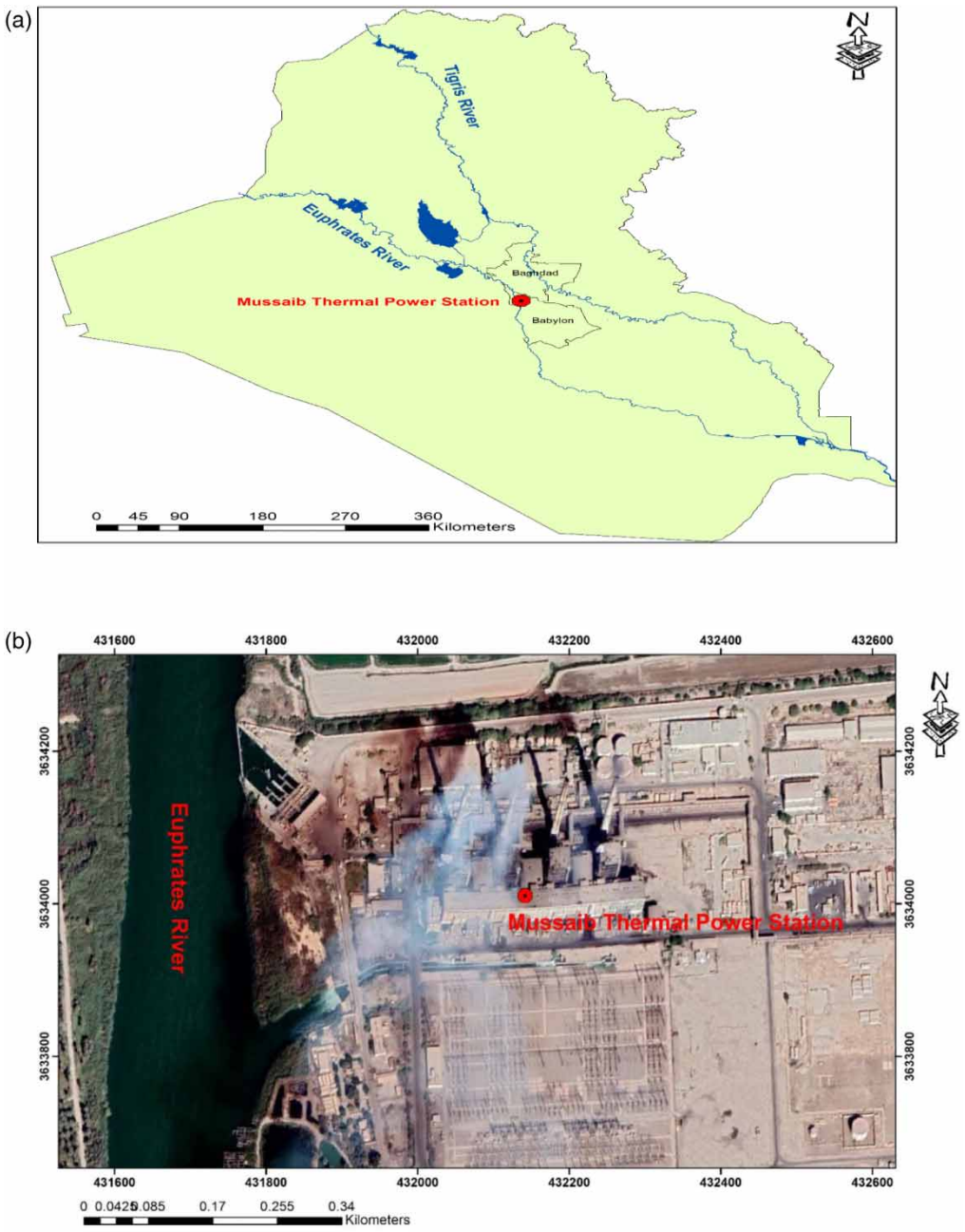

Figure 1 | (a) and (b) Area of case study.

2.2. Numerical modelling

The numerical model of the behavior of the water properties is a set of partial differential equations. These properties will be sited to obtain algebraical equations which can be solved by use of numerical solutions. Equations must be set with a proper of boundary conditions. The equations that formulate problems of the behavior of the water properties in water bodies according to Roberson & Crowe (1997), Babartutsi & Chu (1998) and Nasir *et al.* (2013) are shown below.

2.2.1. Momentum conservation equations

The equation of horizontal momentum:

$$\rho\frac{\partial u}{\partial t}+u\frac{\partial \rho u}{\partial x}+w\frac{\partial \rho u}{\partial z}=\frac{\partial}{\partial x}\left[\mu\frac{\partial u}{\partial x}\right]+\frac{\partial}{\partial z}\left[\mu\frac{\partial u}{\partial z}\right]-\frac{\partial p}{\partial x}+\rho g \tag{1}$$

The equation of vertical momentum:

$$\rho\frac{\partial w}{\partial t}+u\frac{\partial \rho w}{\partial x}+w\frac{\partial \rho w}{\partial z}=\frac{\partial}{\partial x}\left[\mu\frac{\partial w}{\partial x}\right]+\frac{\partial}{\partial z}\left[\mu\frac{\partial w}{\partial z}\right]-\frac{\partial p}{\partial z}+\rho g \tag{2}$$

2.2.2. Thermal energy equation

$$\rho\frac{\partial T}{\partial t}+u\frac{\partial \rho T}{\partial x}+w\frac{\partial \rho T}{\partial z}=\frac{\partial}{\partial x}\left[\frac{\mu}{\sigma}\frac{\partial T}{\partial x}\right]+\frac{\partial}{\partial z}\left[\frac{\mu}{\sigma}\frac{\partial T}{\partial z}\right]-\frac{\alpha(T-T_r)}{c_p * H} \tag{3}$$

2.2.3. Turbulence kinetic equation

$$\rho\frac{\partial k}{\partial t}+u\frac{\partial \rho k}{\partial x}+w\frac{\partial \rho k}{\partial z}=\frac{\partial}{\partial x}\left[\frac{\mu}{\sigma_k}\frac{\partial k}{\partial x}\right]+\frac{\partial}{\partial z}\left[\frac{\mu}{\sigma_k}\frac{\partial k}{\partial z}\right]+G-\rho\varepsilon \tag{4}$$

2.2.4. Dissipation rate equation

$$\rho\frac{\partial \varepsilon}{\partial t}+u\frac{\partial \rho \varepsilon}{\partial x}+w\frac{\partial \rho \varepsilon}{\partial z}=\frac{\partial}{\partial x}\left[\frac{\mu}{\sigma_\varepsilon}\frac{\partial \varepsilon}{\partial x}\right]+\frac{\partial}{\partial z}\left[\frac{\mu}{\sigma_\varepsilon}\frac{\partial \varepsilon}{\partial z}\right]+c_1\frac{\varepsilon}{k}G-c_2\rho\frac{\varepsilon}{k} \tag{5}$$

2.2.5. Temperature–density distribution

$$\rho = 1000.1+0.0182T-0.0055T^2 \tag{6}$$

$$\Phi = c_p.v.\rho.\Delta T \tag{7}$$

2.2.6. Temperature–viscosity distribution

$$\mu = c_M.\rho\left(\frac{k^2}{\varepsilon}\right)\Delta T \tag{8}$$

2.3. Numerical model solution

2.3.1. Numerical solution

The finite difference technique was used to solve partial differential equations. Some assumptions were used in transforming those equations, from the non-linear to the linear equations (Smith 1985; Vincenzo & Gauss 1998). Formulation and simplification of these equations in a two-dimensional numerical model were achieved by using the Alternative Direction Implicit-Explicit method (ADI) with up winding technique. The resulting linear equations were solved using the Gauss-elimination method. Fortran language was the computer program used.

2.3.2. Input data

The input data needed to operate the model and run the computer program are the long reach of the river, depth, hydraulic river properties (such as slope and roughness), time interval and the total time of the study, as well as the temperature of the boiler water, which were obtained from (ECSDIP 2010).

2.3.3. Boundary conditions

The conditions are:

- u = upper value (at the river surface)
- u = zero (at river bottom)
- w = zero (at all points in the horizontal and vertical plane)

Turbulent viscosity (μ) and the rate of dissipation (ε) in the river were obtained from the equations below (Vincenzo & Gauss 1998):

$$\mu = 0.077 \rho u f h \tag{9}$$

$$uf = (GRS)^{1/2} \tag{10}$$

$$\varepsilon = s * g * u \tag{11}$$

Using initial conditions of (μ) and (ε) as calculated from Equations (8) and (10), the initial conditions for the turbulence kinetic energy (K) in the river can be obtained from Equation (8).

The boundary conditions used in the computer program are:

1. In the upstream boundary:

   at $X = 0$, $0 < Z < D$ in which (W, U, T, K, ε) are constants, and D is the depth of the river.

2. In the downstream boundary:

   t $X = L$ and $0 < Z < D$, gradient of W, U, T, K and ε is assumed equal to 0, where L represents the river length.

$$\frac{\partial}{\partial X}(w, u, T, k, \varepsilon) = 0 \tag{12}$$

3. In the boundary surface: $0 < X < L$, and $Z = 0$, W = 0, the gradient of U, K and ε were assumed equal to 0:

$$\frac{\partial}{\partial Z}(u, k, \varepsilon) = 0 \tag{13}$$

4. In the boundary bottom:

   That $0 < X < L$, $Z = D$, $W = 0$, gradient of (T, U, K ε) are equal to 0:

$$\frac{\partial}{\partial Z}(u, T, k, \varepsilon) = 0 \tag{14}$$

2.4. Field works and validation of the model

Observed data of the water properties under consideration in the Euphrates River were obtained from Mussaib Thermal Station. Other data regarding this river were obtained from ECSDIP (2010). Model validation was carried out by a comparison of the observed data with only one period of the predicted results, obtained from the model. The results of this comparison are shown in Figure 2(a) and 2(b).

3. RESULTS AND DISCUSSION

The effect of the hydraulics river parameters along the longitudinal and vertical distribution of water properties, such as density and viscosity, were studied. The results were taken at boiler water temperature equal to 48 °C at the outfall stream, and at the downstream water temperature equal to 30 °C at 500 m length reach of Euphrates river.

3.1. Statistical analysis

Statistical analysis to compare predicted density and observed density such as Chi-square (Equation (15)) and RMSE (Equation (16)), by applying these tests (James 2019). The value of Chi-square computed equal to 0.006514 and Chi-square from table equal to 7.814 with a level of significance of 5% and degree of freedom equal to 3 with a probability of 95%, it is accepted. Regarding RMSE equal to 0.00000655496, it is close to zero. Also, a comparison between predicted viscosity and observed viscosity shows that the value of computed Chi-square equal to 0.005702649, and the Chi-square value from table equal to 7.814 with a level of significance

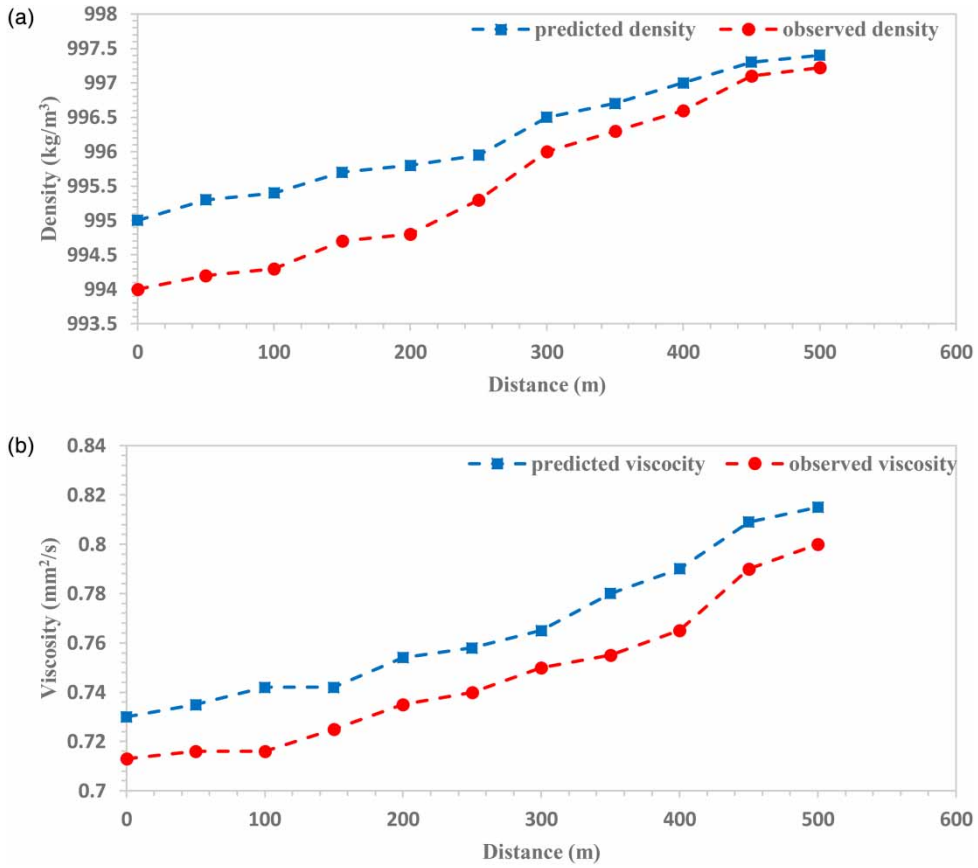

Figure 2 | (a) Comparison between the observed data from the Euphrates River and the predicted data from the model for water density. (b) Comparison between the observed data from the Euphrates River and the predicted data from the model for water viscosity.

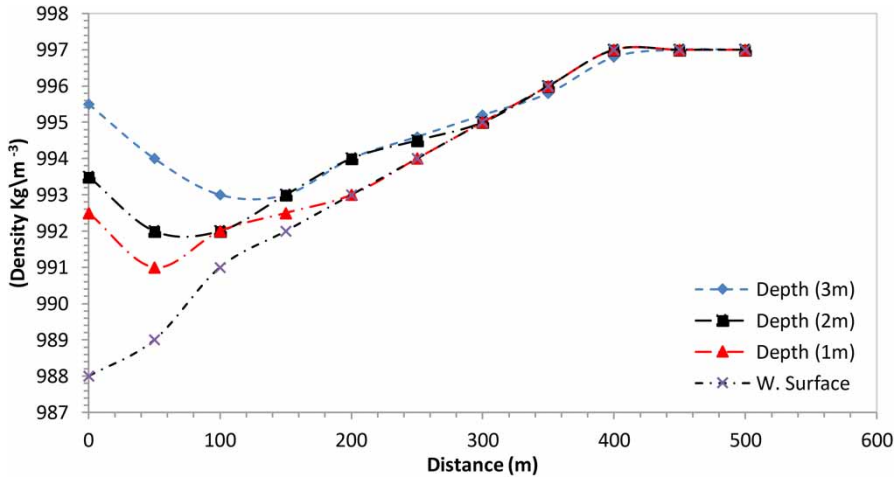

Figure 3 | Effect of bed roughness ($n = 0.04$) in water density at different depths.

of 5% and degree of freedom equal to 3, it is accepted regarding RMSE equal to 0.007895422, it is close to zero:

$$\chi^2 = \sum_{i=1}^{K} \frac{(Q_0 - Q_C)^2}{Q_C} \tag{15}$$

$$RMSE = \sum \left[\frac{Q_o - Q_c}{Q_o}\right]^2 \tag{16}$$

3.2. Prediction of water density values in the study area

Figures 3 and 4 show the impact of roughness bed on the water density values due to boiler water. In these figures, increasing the roughness causes retardation in the density depletion in the longitudinal direction due to a decrease in river velocity. For example, the longitudinal density depletion extends to 350 m downstream of the outfall in the case of $n = 0.04$ m, while it has reached 300 m distance from the outfall in the case of

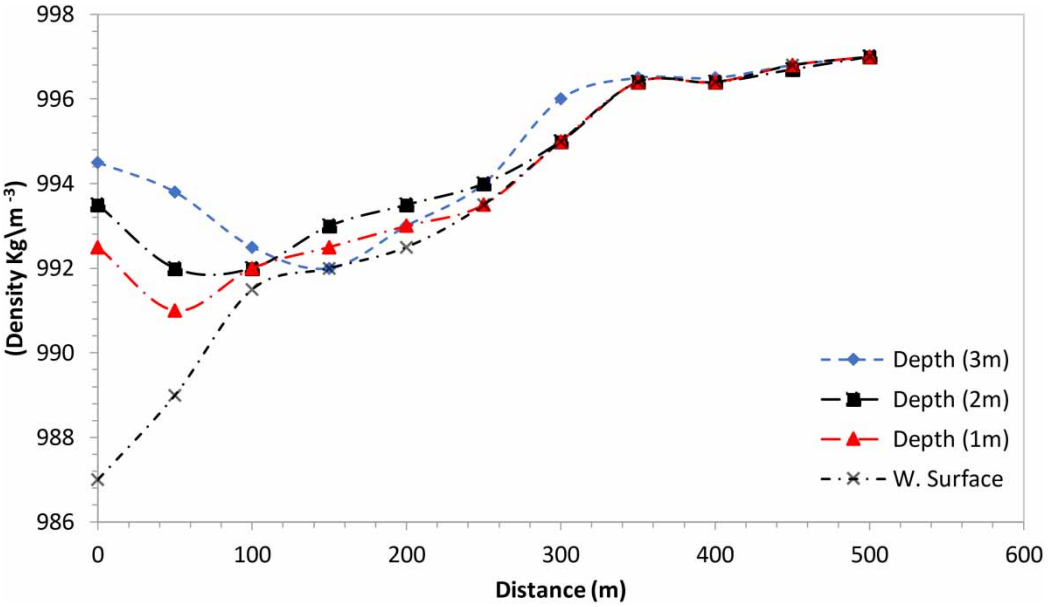

Figure 4 | Effect of bed roughness ($n = 0.12$) in water density at different depths.

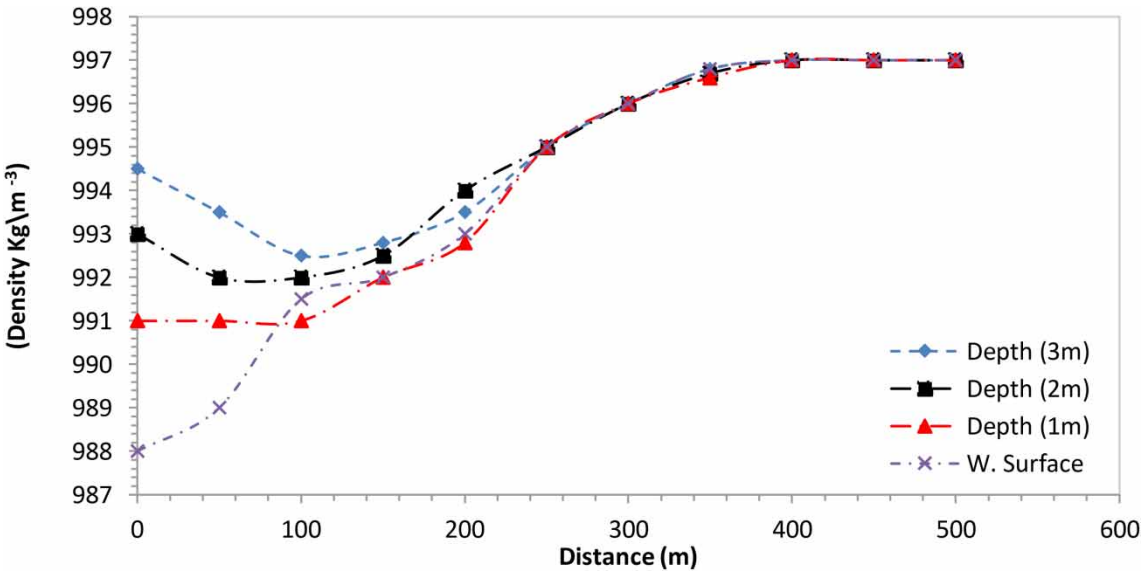

Figure 5 | Effect of water surface slope ($S = 6$ cm/km) on density at different depths.

$n = 0.12$ m. This is because increasing the roughness height causes the advance of water density depletion toward the bottom below the outfall. For example, at a depth of 3 m the density reached 999.5 kg/m^3 when $n = 0.04$ m, while at the same depth, the density reached 994.5 kg/m^3 when $n = 0.12$ m.

Figures 5 and 6 show the effect of the water surface slope on the behavior of water density values due to boiler water. From these figures, it can be seen that increasing of the water surface slope will cause an advance in water density depletion in the longitudinal direction due to an increase in the river velocity. For example, at depths of 3 and 300 m along the reach study, density water had reached 996 kg/m^3 in length in the case of $S = 6$ cm/km, while at the same length, it had reached 995 kg/m^3 in the case of $S = 12$ cm/km. For example, at a depth of 3 m the water density reached 994.5 kg/m^3 at $S = 6$ cm/km, and at the same depth, it reached 996 kg/m^3 at $S = 12$ cm/km. This can be attributed to the effect of buoyancy force which increases vertical diffusion with the increase in water surface slope.

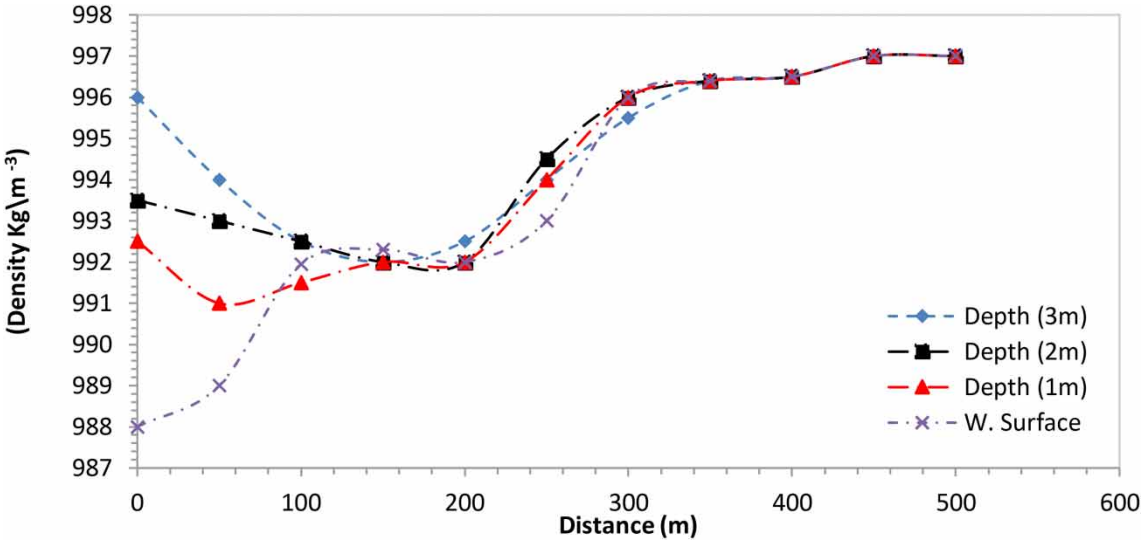

Figure 6 | Effect of water surface slope ($S = 12$ cm/km) on water density at different depths.

3.3. Prediction of water viscosity values in the study area

Figures 7 and 8 show the effect of roughness height on the viscosity due to boiler water. For Figures 7 and 8, increasing the roughness height causes retardation in the water viscosity depletion at the longitudinal direction due to a decrease in river velocity. For example, the longitudinal viscosity extends to 370 m downstream of the outfall in the case of $n = 0.04$ m, while it has reached 300 m. The distance from the outfall in the case of $n = 0.12$ m, on the other hand, increasing the roughness height causes the advance of viscosity depletion toward the bottom below the outfall. For example, at a depth of 3 m the viscosity values had reached 0.7513 mm^2/s when $n = 0.04$ m, while at the same depth, the density had reached 0.7223 mm^2/s when $n = 0.12$ m.

Figures 9 and 10 show the effect of change in the water surface slope at the water viscosity depletion due to boiler water. From Figures 9 and 10 it can be seen that the increase of the slope in water surface will cause an advance in water viscosity depletion at the longitudinal direction due to the increase in the river velocity. For example, at depths of 3 and 300 m along the reach study, viscosity had reached 0.761 mm^2/s in length in the case of $S = 6$ cm/km, while at the same length, it had reached 0.705 mm^2/s in the case of $S = 12$ cm/km. Increasing the water surface slope causes vertical retardation in viscosity values below the outfall. For example, at a depth of 3 m, the water viscosity reached 0.710 mm^2/s at $S = 6$ cm/km. For the same depth, it reached 0.752 mm^2/s at $S = 12$ cm/km.

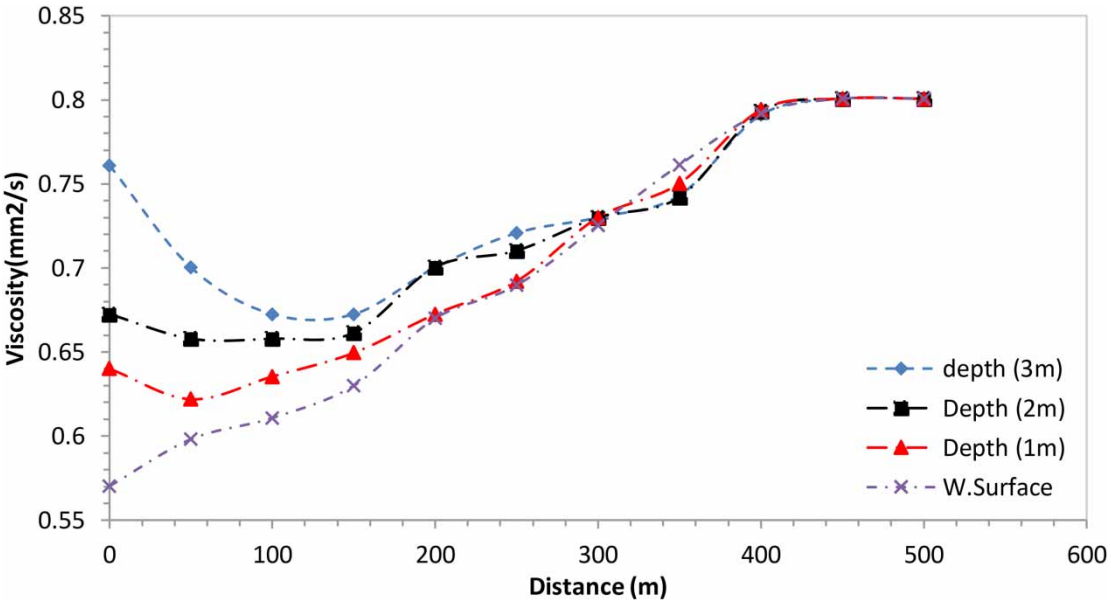

Figure 7 | Effect of bed roughness ($n = 0.04$) in water viscosity at different depths.

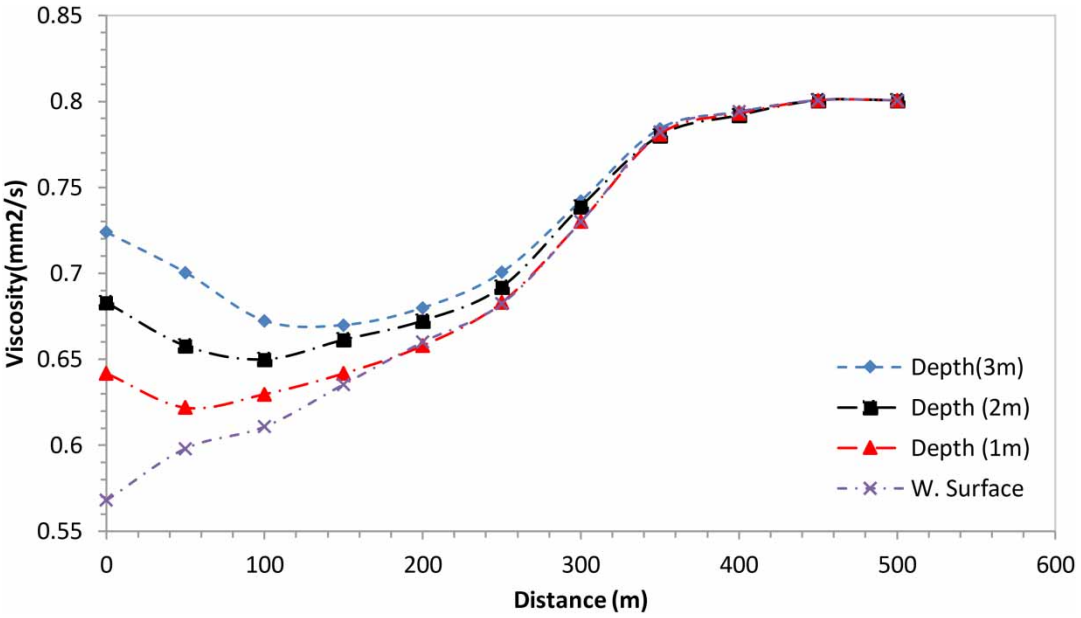

Figure 8 | Effect of bed roughness ($n = 0.12$) in water viscosity at different depths.

4. CONCLUSIONS

The numerical model was verified by the agreement of the model results for density and viscosity with those observed from the Euphrates River according to statistical tests such as Chi-square with the degree of freedom = 3 to both properities above, RMSE was found to be 6.55496×10^{-6} and 0.007895422 for density and viscosity respectively where they are close to zero and another test p-value was found to be 95%.

The height of roughness of the river bed has an impact on the behavior of the water properties distribution as density and viscosity in the rivers, which increases the height of roughness from 0.04 to 0.12 m, causing the longitudinal retardations of density and viscosity depletion of about 26 and 22% and vertical advance of about 14 and 12% respectively

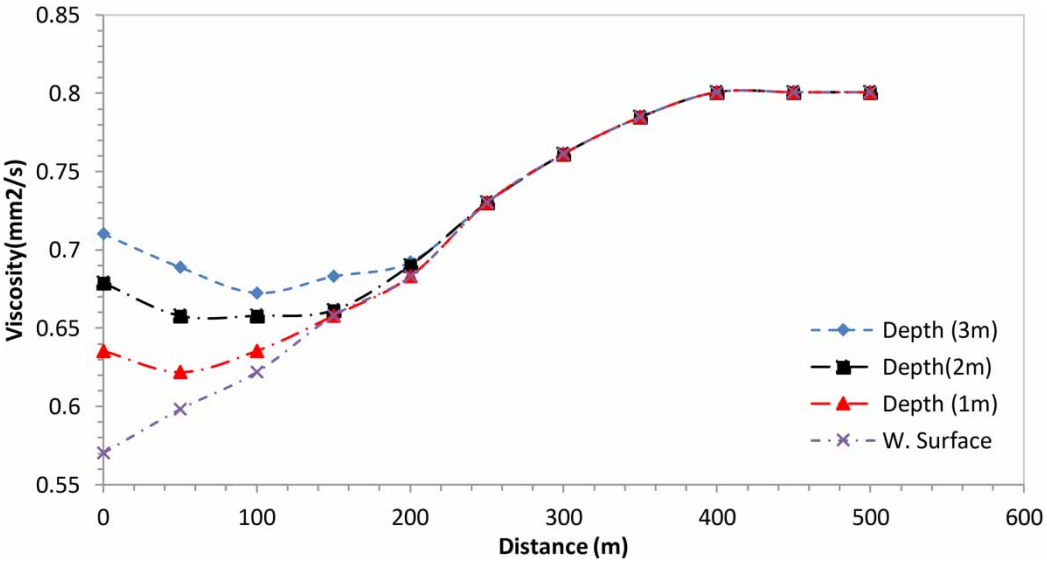

Figure 9 | Effect of the water surface slope ($S = 6$ cm/km) in water viscosity for different depths.

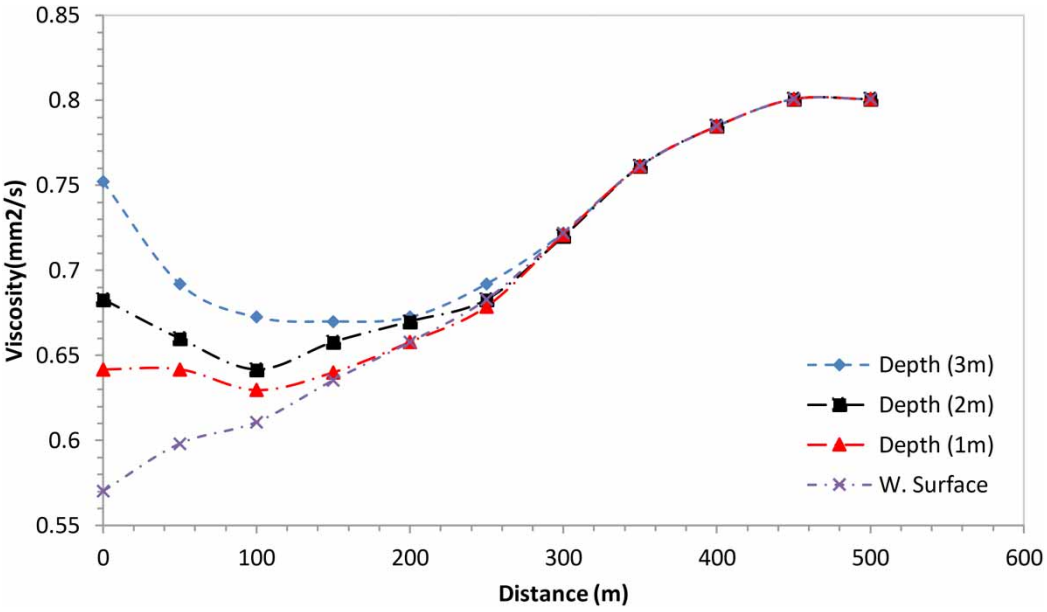

Figure 10 | Effect of the water surface slope ($S = 12$ cm/km) in water viscosity for different depths.

The water surface slope has an impact on the behavior of water properties distribution (such as density and viscosity) of the river. The increasing in slope from 6 to 12 cm/km causes vertical retardation of density and viscosity of about 16 and 13% and the longitudinal advance of depletion of about 19 and 12% respectively.

ACKNOWLEDGEMENTS

The authors are grateful to the Al-Furat Al-Awsat Technical University, Southern Technical University and Al-Mussaib power station, Iraq for their support.

DATA AVAILABILITY STATEMENT

Data cannot be made publicly available; readers should contact the corresponding author for details.

CONFLICT OF INTEREST

The authors declare there is no conflict.

REFERENCES

Abidalla, W. A., Naser, A. S. & Nasir, M. J. 2022 Finding of suitable transportation rate formula by using 'velocity-height-distance' for bed material load. *Mathematical Modelling of Engineering Problems* **9**(2), 463–467. https://doi.org/10.18280/mmep.090223.

APHA 2011 *Standard Method of the Examination of Water and Wastewater*. APA, Washington, DC.

Babartutsi, S. & Chu, V. H. 1998 Modelling transverse mixing layer in shallow open channel flows. *Journal of Hydraulic Engineering* **124**(10), 1059–1063.

Behrens, P., Van Vliet, M. T. H., Nanninga, T., Walsh, B. & Rodrigues, J. F. D. 2017 Climate change and the vulnerability of electricity generation to water stress in the European Union. *Nature Energy* **2**, 17114.

ECSDIP 2010 *Euphrates Company for Studying and Design of Irrigation Projects, Tigris River Training Inside Baghdad City*. Scientific Research Publishing, Baghdad, Iraq.

EPA 2001 *State of the Environmental Report for Thames Region, First Update*. Environment Agency, Bristol.

James, N. 2019 *Complete Probability & Statistical 1 for Cambridge International AS &A Level*, 2nd edn. OUP, Oxford.

Kalinowska, M. P. & Rowinski, P. M. 2012 Uncertainty in computations of the of warm water in a river – lessons from environmental impact assessment case study. *Hydrology Earth System Science* **16**, 4177–4190. doi:10.5194/hess-16-4177-2012.

Kalinowska, M. P. & Rowinski, P. M. 2015 *Modelling of the Spread of Thermal Pollution in Rivers with Limited Data*. CRC Press, London. doi:10.1201/b17133-32-2015.

Macknick, J., Zhou, E., Miara, A., Ibanez, E., O'Connell, M., Hummon, M. & Brinkman, G. 2016 *Water and Climate Impacts on Power System Operations: The Importance of Cooling Systems and Demand Response Measures*. NREL/TP-6A20-66714. National Renewable Energy Laboratory, U.S. Department of Energy Office of Energy Efficiency & Renewable Energy, Washington, DC, USA.

Miaral, A., Charles, O., Vincent, C., Balazs, F., Fabio, C. & Robin, N. 2018 Thermal pollution impacts on rivers and power supply in the Mississippi River watershed. *Environmental Research Letters* **13**(3), 034033.

Nasir, M. J., Gzar, H. A. & Guhulam, S. H. 2013 Numerical modelling for prediction of the dissolved oxygen depletion affected by boiler water discharged in rivers. *Journal of Engineering and Development* **17**(4), 101–113.

Nasir, M. J., Abdulhasan, M. J., Abbas Ridha, S. Z., Khalid, S. H. & Jasim, H. M. 2022 Statistical assessment for performance of Al-Mussaib drinking water treatment plant at the year 2020. *Water Practice & Technology* **17**(3), 808–8016. doi:10.2166/wpt.2022.020.

Roberson, J. A. & Crowe, C. T. 1997 *Engineering Fluid Mechanics*. John Wiley and Sons, Inc, New York, USA.

Smith, G. D. 1985 *Numerical Solution of Partial Differential Equations – Finite Difference Methods*. Oxford University Press, Oxford, UK.

Vincenzo, C. & Gauss, S. 1998 Numerical simulation of 3D quasi-hydrostatic, free surface flows. *Journal of Hydraulic Division* **124**(7), 678–686.

First received 31 March 2023; accepted in revised form 12 June 2023. Available online 14 July 2023